

---

# Geometric Algebra Transformers

---

Johann Brehmer

Pim de Haan

Sönke Behrends

Taco Cohen

Qualcomm AI Research\*

{jbrehmer, pim, sbehrend, tacos}@qti.qualcomm.com

## Abstract

Problems involving geometric data arise in a variety of fields, including computer vision, robotics, chemistry, and physics. Such data can take numerous forms, such as points, direction vectors, planes, or transformations, but to date there is no single architecture that can be applied to such a wide variety of geometric types while respecting their symmetries. In this paper we introduce the Geometric Algebra Transformer (GATr), a general-purpose architecture for geometric data. GATr represents inputs, outputs, and hidden states in the projective geometric algebra, which offers an efficient 16-dimensional vector space representation of common geometric objects as well as operators acting on them. GATr is equivariant with respect to  $E(3)$ , the symmetry group of 3D Euclidean space. As a transformer, GATr is scalable, expressive, and versatile. In experiments with  $n$ -body modeling and robotic planning, GATr shows strong improvements over non-geometric baselines.

## 1 Introduction

From molecular dynamics to astrophysics, from material design to robotics, fields across science and engineering deal with geometric data: points, directions, surfaces, orientations, and so on. The geometric nature of data provides a rich structure: a notion of common operations between geometric types (computing distances between points, applying rotations to orientations, etc.), a well-defined behaviour of data under transformations of a system, and the independence of certain properties of coordinate system choices.

When learning relations from geometric data, incorporating this rich structure into the architecture has the potential to improve the performance, especially in the low-data regime. To implement such an inductive bias, it is useful to first categorize inputs, outputs, and internal data into certain object types, for instance group representations. Next, the functions mapping between these types have certain regularity constraints imposed, for instance based on equivariance [8].

In this spirit, we introduce the *Geometric Algebra Transformer* (GATr), a general-purpose network architecture for geometric data. GATr brings together three key ideas.

**Geometric algebra:** To naturally describe both geometric objects as well as their transformations in three-dimensional space, GATr represents data as multivectors of the projective geometric algebra  $\mathbb{G}_{3,0,1}$ . Geometric algebra is an elegant, versatile and practical mathematical framework for geometrical computations. The particular algebra  $\mathbb{G}_{3,0,1}$  extends the vector space  $\mathbb{R}^3$  to 16-dimensional multivectors, which can natively represent various geometric types and  $E(3)$  poses. In this framework, common interactions between geometric data types can be computed with few operations, in particular the geometric product.

**Equivariance:** To behave consistently under transformations, GATr is equivariant with respect to  $E(3)$ , the symmetry group of three-dimensional space. To this end, we develop several new  $E(3)$ -equivariant primitives mapping between multivectors, including equivariant linear maps, an attention mechanism, nonlinearities, and normalization layers.

---

\*Qualcomm AI Research is an initiative of Qualcomm Technologies, Inc.

**Transformer:** Due to its favorable scaling properties, expressiveness, trainability, and versatility, the transformer architecture [42] has become the de-facto standard for a wide range of problems. GATr is based on the transformer architecture, and hence inherits these benefits.

GATr hence combines two lines of research: the representation of geometric objects with geometric algebra [16, 17, 32], popular in computer graphics and physics and recently gaining traction in deep learning [5, 35, 40], and the encoding of symmetries through equivariant deep learning [12]. The result—to the best of our knowledge the first  $E(3)$ -equivariant architecture with internal geometric algebra representations<sup>2</sup>—is a versatile network for problems involving geometric data.

We demonstrate GATr in two problems from entirely different fields: predicting  $n$ -body trajectories and planning robotic motion, using GATr as the backbone of an  $E(3)$ -invariant diffusion model. In both cases, GATr significantly outperforms non-geometric baselines.

## 2 Background

**Geometric algebra** We begin with a brief overview of geometric algebra (GA); for more detail, see e. g. Refs. [16, 17, 32, 35]. Whereas a plain vector space like  $\mathbb{R}^3$  allows us to take linear combinations of elements  $x$  and  $y$  (vectors), a geometric algebra additionally has a bilinear associative operation: the *geometric product*, denoted simply by  $xy$ . By multiplying vectors, one obtains so-called *multivectors*, which can represent both geometrical *objects* and *operators*. Like vectors, multivectors have a notion of direction as well as magnitude and orientation (sign), and can be linearly combined.

Multivectors can be expanded on a multivector basis, consisting of products of basis vectors. For example, in a 3D GA with orthogonal basis  $e_1, e_2, e_3$ , a general multivector takes the form

$$x = x_s + x_1 e_1 + x_2 e_2 + x_3 e_3 + x_{12} e_1 e_2 + x_{13} e_1 e_3 + x_{23} e_2 e_3 + x_{123} e_1 e_2 e_3, \quad (1)$$

with real coefficients  $(x_s, x_1, \dots, x_{123}) \in \mathbb{R}^8$ . Thus, similar to how a complex number  $a + bi$  is a sum of a real scalar and an imaginary number,<sup>3</sup> a general multivector is a sum of different kinds of elements. These are characterized by their dimensionality (grade), such as scalars (grade 0), vectors  $e_i$  (grade 1), bivectors  $e_i e_j$  (grade 2), all the way up to the *pseudoscalar*  $e_1 \cdots e_d$  (grade  $d$ ).

The geometric product is characterized by the fundamental equation  $vv = \langle v, v \rangle$ , where  $\langle \cdot, \cdot \rangle$  is an inner product. In other words, we require that the square of a vector is its squared norm. In an orthogonal basis, where  $\langle e_i, e_j \rangle \propto \delta_{ij}$ , one can deduce that the geometric product of two different basis vectors is antisymmetric:  $e_i e_j = -e_j e_i$ .<sup>4</sup> Since reordering only produces a sign flip, we only get one basis multivector per unordered subset of basis vectors, and so the total dimensionality of a GA is  $\sum_{i=0}^d \binom{d}{k} = 2^d$ . Moreover, using bilinearity and the fundamental equation one can compute the geometric product of arbitrary multivectors.

The symmetric and antisymmetric parts of the geometric product are called the interior and exterior (wedge) product. For vectors  $x$  and  $y$ , these are defined as  $\langle x, y \rangle = (xy + yx)/2$  and  $x \wedge y \equiv (xy - yx)/2$ . The former is indeed equal to the inner product used to define the GA, whereas the latter is new notation. Whereas the inner product computes the similarity, the exterior product constructs a multivector (called a blade) representing the weighted and oriented subspace spanned by the vectors. Both operations can be extended to general multivectors [17].

The final primitive of the GA that we will require is the dualization operator  $x \mapsto x^*$ . It acts on basis elements by swapping “empty” and “full” dimensions, e. g. sending  $e_1 \mapsto e_{23}$ .

**Projective geometric algebra** In order to represent three-dimensional objects as well as arbitrary rotations and translations acting on them, the 3D GA is not enough: as it turns out, its multivectors can only represent linear subspaces passing through the origin as well as rotations around it. A common trick to expand the range of objects and operators is to embed the space of interest (e.g.  $\mathbb{R}^3$ ) into a higher dimensional space whose multivectors represent more general objects and operators in the original space.

---

<sup>2</sup>Concurrently to our work, a similar network architecture was studied by Ruhe et al. [34]; in a future version of this manuscript we will comment on similarities and differences.

<sup>3</sup>Indeed the imaginary unit  $i$  can be thought of as the bivector  $e_1 e_2$  in a 2D GA.

<sup>4</sup>The antisymmetry can be derived by using  $v^2 = \langle v, v \rangle$  to show that  $e_i e_j + e_j e_i = (e_i + e_j)^2 - e_i^2 - e_j^2 = 0$ .

Object / operator	Scalar	Vector	Bivector	Trivector	PS		
	1	$e_0$	$e_i$	$e_{0i}$	$e_{ij}$	$e_{0ij}$	$e_{123}$
Scalar $\lambda \in \mathbb{R}$	$\lambda$	0	0	0	0	0	0
Plane w/ normal $n \in \mathbb{R}^3$ , origin shift $d \in \mathbb{R}$	0	$d$	$n$	0	0	0	0
Line w/ direction $n \in \mathbb{R}^3$ , orthogonal shift $s \in \mathbb{R}^3$	0	0	0	$s$	$n$	0	0
Point $p \in \mathbb{R}^3$	0	0	0	0	0	$p$	1
Pseudoscalar $\mu \in \mathbb{R}$	0	0	0	0	0	0	$\mu$
Reflection through plane w/ normal $n \in \mathbb{R}^3$ , origin shift $d \in \mathbb{R}$	0	$d$	$n$	0	0	0	0
Translation $t \in \mathbb{R}^3$	1	0	0	$\frac{1}{2}t$	0	0	0
Rotation expressed as quaternion $q \in \mathbb{R}^4$	$q_0$	0	0	0	$q_i$	0	0
Point reflection through $p \in \mathbb{R}^3$	0	0	0	0	0	$p$	1

Table 1: Embeddings of common geometric objects and transformations into the projective geometric algebra  $\mathbb{G}_{3,0,1}$ . The columns show different components of the multivectors with the corresponding basis elements, with  $i, j \in \{1, 2, 3\}$ ,  $j \neq i$ , i.e.  $ij \in \{12, 13, 23\}$ . For simplicity, we fix gauge ambiguities (the weight of the multivectors) and leave out signs (which depend on the ordering of indices in the basis elements).

In this paper we work with the projective geometric algebra  $\mathbb{G}_{3,0,1}$  [16, 32, 35]. Here one adds a fourth *homogeneous coordinate*  $x_0 e_0$  to the vector space, yielding a  $2^4 = 16$ -dimensional geometric algebra. The metric of  $\mathbb{G}_{3,0,1}$  is such that  $e_0^2 = 0$  and  $e_i^2 = 1$  for  $i = 1, 2, 3$ . As we will explain in the following, in this setup the 16-dimensional multivectors can represent 3D points, lines, and planes, which need not pass through the origin, and arbitrary rotations, reflections, and translations in  $\mathbb{R}^3$ .

**Representing transformations** In geometric algebra, a vector  $u$  can act as an operator, reflecting other elements in the hyperplane orthogonal to  $u$ . Since any orthogonal transformation is equal to a sequence of reflections, this allows us to express any such transformation as a geometric product of (unit) vectors, called a (unit) *versor*  $u = u_1 \cdots u_k$ . Furthermore, since the product of unit versors is a unit versor, and unit vectors are their own inverse ( $u^2 = 1$ ), these form a group called the Pin group associated with the metric. Similarly, products of an even number of reflections form the Spin group. In the projective geometric algebra  $\mathbb{G}_{3,0,1}$ , these are the double cover<sup>5</sup> of  $E(3)$  and  $SE(3)$ , respectively. We can thus represent any rotation, translation, and mirroring—the symmetries of three-dimensional space—as  $\mathbb{G}_{3,0,1}$  multivectors.

In order to apply a versor  $u$  to an arbitrary element  $x$ , one uses the *sandwich product*:

$$\rho_u(x) = \begin{cases} uxu^{-1} & \text{if } u \text{ is even} \\ u\hat{x}u^{-1} & \text{if } u \text{ is odd} \end{cases} \quad (2)$$

Here  $\hat{x}$  is the *grade involution*, which flips the sign of odd-grade elements such as vectors and trivectors, while leaving even-grade elements unchanged. Equation 2 thus gives us a linear action (i.e. group representation) of the Pin and Spin groups on the  $2^d$ -dimensional space of multivectors. The sandwich product is grade-preserving, so this representation splits into a direct sum of representations on each grade.

**Representing 3D objects** Following Refs. [16, 32, 35], we represent planes with vectors, and require that the intersection of two geometric objects is given by the wedge product of their representations. Lines (the intersection of two planes) are thus represented as bivectors, points (the intersection of three planes) as trivectors. This leads to a duality between objects and operators, where objects are represented like transformations that leave them invariant. Table 1 provides a dictionary of these embeddings. It is easy to check that this representation is consistent with using the sandwich product for transformations.

**Equivariance** We construct network layers that are equivariant with respect to  $E(3)$ , or equivalently its double cover  $\text{Pin}(3, 0, 1)$ . A function  $f : \mathbb{G}_{3,0,1} \rightarrow \mathbb{G}_{3,0,1}$  is  $\text{Pin}(3, 0, 1)$ -equivariant with respect to the representation  $\rho$  (or  $\text{Pin}(3, 0, 1)$ -equivariant for short) if

$$f(\rho_u(x)) = \rho_u(f(x)) \quad (3)$$

for any  $u \in \text{Pin}(3, 0, 1)$  and  $x \in \mathbb{G}_{3,0,1}$ , where  $\rho_u(x)$  is the sandwich product defined in Eq. (2).

<sup>5</sup>This means that for each element of  $E(3)$  there are two elements of  $\text{Pin}(3, 0, 1)$ , e.g. both the vector  $v$  and  $-v$  represent the same reflection.

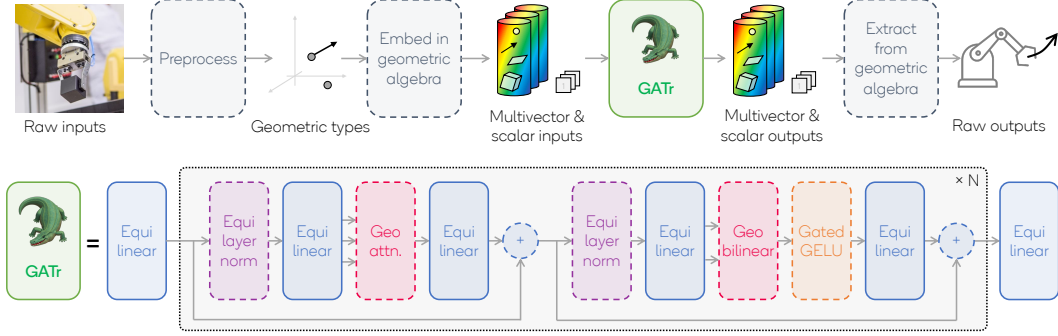


Figure 1: Overview over the GATr architecture. Boxes with solid lines are learnable components, those with dashed lines are fixed.

### 3 The Geometric Algebra Transformer

#### 3.1 Design principles and architecture overview

**Geometric inductive bias through geometric algebra representations** GATr is designed to provide a strong inductive bias for geometric data. It should be able to represent different geometric objects and their transformations, for instance points, lines, planes, translations, rotations, and so on. In addition, it should be able to represent common interactions between these types with few layers, and be able to identify them from little data (while maintaining the low bias of large transformer models). Examples of such common patterns include computing the relative distances between points, moving objects along directions, or computing the intersections of planes and lines.

Following a body of research in computer graphics, we propose that geometric algebra gives us a language that is well-suited to this task. We use the projective geometric algebra  $\mathbb{G}_{3,0,1}$  and use the plane-based representation of geometric structure outlined in the previous section.

**Symmetry awareness through  $E(3)$  equivariance** Our architecture should respect the symmetries of 3D space. Therefore we design GATr to be equivariant with respect to the symmetry group  $E(3)$  of translations, rotations, and reflections. Since we represent data in the projective geometric algebra  $\mathbb{G}_{3,0,1}$ , we can represent objects that transform arbitrarily under  $E(3)$ , including with respect to translations of the inputs. This is in stark contrast with most  $E(3)$ -equivariant architectures, whose features only transform under rotation, and which must handle points and translations in hand-crafted ways, like by canonicalizing w. r. t. the center of mass or by treating the difference between points as a translation-invariant vector.

Note that many systems will not exhibit the full  $E(3)$  symmetry group. The direction of gravity, for instance, often breaks it down to the smaller  $E(2)$  group. To maximize the versatility of GATr, we choose to develop a  $E(3)$ -equivariant architecture and to include symmetry-breaking as part of the network inputs, similar to how position embeddings break permutation equivariance in transformers.

**Flexibility and expressiveness through axial attention** Finally, GATr should be expressive, easy to train, and be as flexible as possible, supporting variable geometric inputs and both static scenes and time series.

These desiderata motivate us to implement GATr as a transformer [42], based on attention over multiple objects (similar to tokens in MLP or image patches in computer vision). When describing dynamic data, we extend the architecture to an axial transformer [24], with alternating blocks that attend over objects and over time steps.

GATr is thus also equivariant with respect to permutations along the object dimension. As in standard transformers, we break this equivariance along time dimensions through positional embedding.

**Architecture overview** We sketch GATr in Fig. 1. In the top row, we show the overall workflow. If necessary, raw inputs are first preprocessed into geometric types. The geometric objects are then embedded into multivectors of the geometric algebra  $\mathbb{G}_{3,0,1}$ , following the recipe described in Tbl. 1.

The multivector-valued data are processed with a GATr network. We show this architecture in more detail in the bottom row of Fig. 1. GATr consists of  $N$  transformer blocks, each consisting of an equivariant multivector LayerNorm, an equivariant multivector self-attention mechanism, a residual connection, another equivariant LayerNorm, an equivariant multivector MLP with geometric bilinear interactions, and another residual connection. The architecture is thus similar to a typical transformer [42] with pre-layer normalization [1, 46], but adapted to correctly handle multivector data and be  $E(3)$  equivariant. We describe the individual layers below.

Finally, from the outputs of the GATr network we extract the target variables, again following the mapping given in Tbl. 1.

### 3.2 GATr primitives

**Linear layers** We begin with linear layers between multivectors. In Appendix A, we show that the equivariance condition of Eq. (3) severely constrains them:

**Proposition 1.** *Any linear map  $\phi : \mathbb{G}_{d,0,1} \rightarrow \mathbb{G}_{d,0,1}$  that is equivariant to  $\text{Pin}(d, 0, 1)$  is of the form*

$$\phi(x) = \sum_{k=0}^{d+1} w_k \langle x \rangle_k + \sum_{k=0}^d v_k e_0 \langle x \rangle_k \quad (4)$$

for parameters  $w \in \mathbb{R}^{d+2}$ ,  $v \in \mathbb{R}^{d+1}$ . Here  $\langle x \rangle_k$  is the blade projection of a multivector, which sets all non-grade- $k$  elements to zero.

Thus,  $E(3)$ -equivariant linear maps between  $\mathbb{G}_{3,0,1}$  multivectors can be parameterized with nine coefficients, five of which are the grade projections and four include a multiplication with the homogeneous basis vector  $e_0$ . We visualize this basis in Fig. 2. We thus parameterize affine layers between multivector-valued arrays with Eq. (4), with learnable coefficients  $w_k$  and  $v_k$  for each combination of input channel and output channel. In addition, there is a learnable bias term for the scalar components of the outputs (biases for the other components are not equivariant).

**Geometric bilinears** Equivariant linear maps are not sufficient to build expressive networks. The reason is that these operations allow for only very limited grade mixing, as shown in Fig. 2. For the network to be able to construct new geometric features from existing ones, such as the translation vector between two points, two additional primitives are essential.

The first is the geometric product  $x, y \mapsto xy$ , the fundamental bilinear operation of geometric algebra. It allows for substantial mixing between grades: for instance, the geometric product of vectors consists of scalars and bivector components. The geometric product is equivariant (Appendix A).

The second geometric primitive we use is derived from the so-called *join*<sup>6</sup>  $x, y \mapsto (x^* \wedge y^*)^*$ . This map may appear complicated, but it plays a simple role in our architecture: an equivariant map that involves the dual  $x \mapsto x^*$ . Including the dual in an architecture is essential for expressivity: in  $\mathbb{G}_{3,0,1}$ , without any dualization it is impossible to represent even simple functions such as the Euclidean distance between two points [16]; we show this in Appendix A. While the dual itself is not  $\text{Pin}(3, 0, 1)$ -equivariant (w. r. t.  $\rho$ ), the join operation is equivariant to even (non-mirror) transformations. To make the join equivariant to mirrorings as well, we multiply its output with a pseudoscalar derived from the network inputs:  $x, y, z \mapsto \text{EquiJoin}(x, y; z) = z_{0123}(x^* \wedge y^*)^*$ , where  $z_{0123} \in \mathbb{R}$  is the pseudoscalar component of a reference multivector  $z$  (see Appendix B).

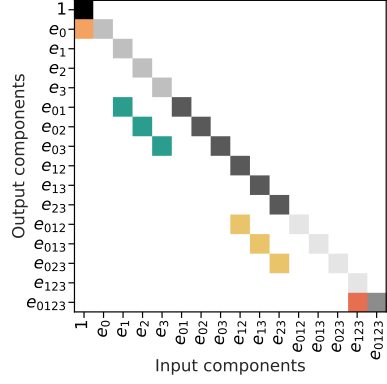


Figure 2: Basis for equivariant linear maps between  $\mathbb{G}_{3,0,1}$  multivectors. Each color visualizes the non-zero components of a different basis map (there is no overlap between the different elements in this basis). The basis maps shown in gray are grade projections, the more colorful ones also left-multiply with  $e_0$ .

<sup>6</sup>Technically, the join has an anti-dual, not the dual, in the output. We leave this detail out for notational simplicity. In our network architecture, it makes no difference for equivariance nor for expressivity whether the anti-dual or dual is used, as any equivariant linear layer can transform between the two.

We define a *geometric bilinear layer* that combines the geometric product and the join of the two inputs as  $\text{Geometric}(x, y; z) = \text{Concatenate}_{\text{channels}}(xy, \text{EquiJoin}(x, y; z))$ . In GATr, this layer is included in the MLP.<sup>7</sup>

**Nonlinearities and normalization** We use scalar-gated GELU nonlinearities [23]  $\text{GatedGELU}(x) = \text{GELU}(x_1)x$ , where  $x_1$  is the scalar component of the multivector  $x$ . Moreover, we define an  $E(3)$ -equivariant LayerNorm operation for multivectors as  $\text{LayerNorm}(x) = x/\sqrt{\mathbb{E}_c \langle x, x \rangle}$ , where the expectation goes over channels and we use the invariant inner product  $\langle \cdot, \cdot \rangle$  of  $\mathbb{G}_{3,0,1}$ .

**Attention** Given multivector-valued query, key, and value tensors, each consisting of  $n_i$  items (or tokens) and  $n_c$  channels (key length), we define the  $E(3)$ -equivariant multivector attention as

$$\text{Attention}(q, k, v)_{i'c'} = \sum_i \text{Softmax}_i \left( \frac{\sum_c \langle q_{i'c}, k_{ic} \rangle}{\sqrt{8n_c}} \right) v_{ic'}. \quad (5)$$

Here the indices  $i, i'$  label items,  $c, c'$  label channels, and  $\langle \cdot, \cdot \rangle$  is the invariant inner product of the geometric algebra. Just as in the original transformer [42], we thus compute scalar attention weights with a scaled dot product; the difference is that we use the inner product of  $\mathbb{G}_{3,0,1}$ .<sup>8,9</sup> We extend this attention mechanism to multi-head self-attention in the usual way.

### 3.3 Extensions

**Auxiliary scalar representations** While multivectors are well-suited to model geometric data, many problems contain non-geometric information as well. Such scalar information may be high-dimensional, for instance in sinusoidal positional encoding schemes. Rather than embedding into the scalar components of the multivectors, we add an auxiliary scalar representation to the hidden states of GATr. Each layer thus has both scalar and multivector inputs and outputs. They have the same batch dimension and item dimension, but may have different number of channels.

This additional scalar information interacts with the multivector data in two ways. In linear layers, we allow the auxiliary scalars to mix with the scalar component of the multivectors. In the attention layer, we compute attention weights both from the multivectors, as given in Eq. (5), and from the auxiliary scalars, using a regular scaled dot-product attention. The two attention maps are summed before computing the softmax, and the normalizing factor is adapted. In all other layers, the scalar information is processed separately from the multivector information, using the unrestricted form of the multivector map. For instance, nonlinearities transform multivectors with equivariant gated GELUs and auxiliary scalars with regular GELU functions. We describe the scalar path of our architecture in more detail in Appendix B.

**Rotary positional embeddings** GATr assumes the data can be described as a set of items (or tokens). If these items are distinguishable and form a sequence, we encode their position using rotary position embeddings [41] in the auxiliary scalar variables.<sup>10</sup>

**Axial attention over objects and time** The architecture is flexible about the structure of the data. In some use cases, there will be a single dimension along which objects are organized, for instance when describing a static scene or the time evolution of a single object. But GATr also supports the organization of a problem along multiple axes, for example with one dimension describing objects and another time steps. In this case, we follow an axial transformer layout [24], alternating between transformer blocks that attend over different dimensions. (The not-attended dimensions in each block are treated like a batch dimension.)

<sup>7</sup>Additional geometric bilinears in the attention block did not improve performance in our experiments.

<sup>8</sup>We also experimented with attention mechanisms that use the geometric product rather than the dot product, but found a worse performance in practice.

<sup>9</sup>Since this dot product of  $\mathbb{G}_{3,0,1}$  only depends on 8 out of 16 multivector dimensions, we scale the inner product by  $\sqrt{8n_c}$  rather than  $\sqrt{16n_c}$  as one would do in a conventional transformer with key dimension  $d_k = 16n_c$ .

<sup>10</sup>Since auxiliary scalar representations and multivectors mix in the attention mechanism, the rotary position embeddings also affect the multivector processing.

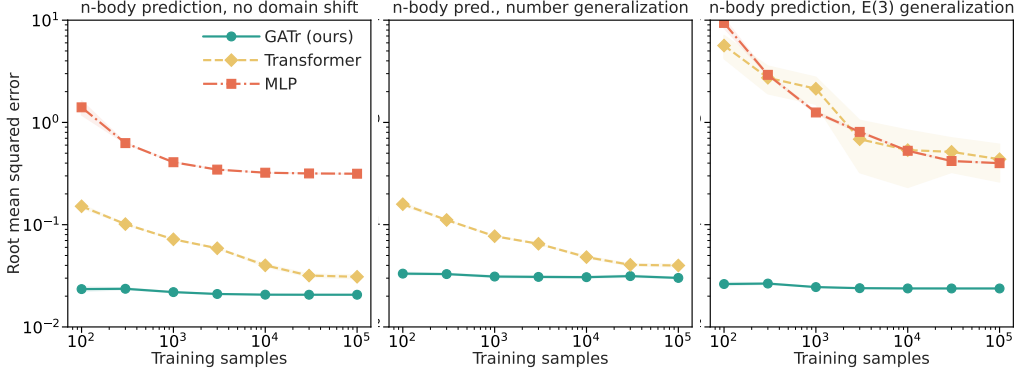


Figure 3: Results on a synthetic  $n$ -body dynamics dataset. We show the error in predicting future positions of planets as a function of the training dataset size. Out of five independent training runs, the mean and standard error are shown. **Left:** Evaluating without distribution shift. GATr (—) is substantially more sample efficient than transformer (---) and MLP (—·—) baselines. **Middle:** Evaluating on systems with more planets than in the training data. Both GATr and the baseline transformer generalize well to different object counts. **Right:** Evaluating on translated data. Because GATr is  $E(3)$  equivariant, it is able to generalize under this domain shift.

## 4 Applications

### 4.1 Planet trajectory prediction

We first demonstrate GATr on a  $n$ -body dynamics prediction problem. Given the masses, initial positions, and velocities of a star and a few planets, the goal is to predict the final position after the system has evolved under Newtonian gravity for some time. We generate synthetic training sets of between 100 and 100 000 samples, consisting of the initial and final state of a star and three planets. There are three evaluation sets of 5 000 samples each: one just like the training data, one with five planets instead of three, and one where the coordinates are translated to a spatial region where the training data had low density. GATr is compared to two baselines: a vanilla transformer and an MLP.<sup>11</sup> We describe the details of the dataset as well as our hyperparameter choices in Appendix C.

In the left panel of Fig. 3 we show the mean squared error in predicting these positions achieved by GATr as a function of the number of training samples used. The MLP, which has the least strong inductive bias and treats the object positions and velocities as a single, structureless feature vector, performs poorly on this task. The transformer structures the data in terms of objects and is permutation-equivariant, but not aware of the geometry; it achieves a reasonable prediction accuracy when using the full training set. Our GATr architecture, however, drastically outperforms both non-equivariant baselines and is able to predict final positions with high accuracy even from just 100 training samples.

GATr also generalizes robustly out of domain, as we show in the middle and right panels of Fig. 1. When evaluated on a larger number of planets, the mean error becomes larger, as non-trivial gravitational interactions become more frequent, but GATr still outperforms the transformer baseline (the MLP does not support the evaluation on different object configurations). As an  $E(3)$ -equivariant architecture, the performance GATr does not drop when evaluated on spatially translated data, while the non-equivariant baselines are less robust to this domain shift.

### 4.2 Robotic planning through invariant diffusion

In our next experiment, we show how GATr defines an  $E(3)$ -invariant diffusion model, that it can be used for model-based reinforcement learning and planning, and that this combination is well-suited to solve robotics problems.

We follow Janner et al. [27], who propose to treat learning a world model and planning within that model as a unified generative modeling problem. After training a diffusion model [38] on offline trajectories, one can use it in a planning loop, sampling from it conditional on the current state, desired future states, or to maximize a given reward, as needed. While this Diffuser method performs well

<sup>11</sup>We will add a comparison to the Geometric Clifford Algebra Networks by Ruhe et al. [35] as soon as their code is public.

empirically, it does not take advantage of the rich geometric structure of the geometric environments that many embodied agents find themselves in.

We use a GATr model as the denoising network in a diffusion model and to use it for planning. We call this combination *GATr-Diffuser*. GATr is equivariant with respect to  $E(3)$  and the object permutation group  $S_n$ . When used together with a base density that is  $E(3) \times S_n$ -invariant, the diffusion model is also  $E(3) \times S_n$ -invariant [4, 28]. Often, a particular task requires breaking this symmetry: imagine, for instance, that a particular object needs to be moved to a particular location. The Diffuser approach is an excellent match for such situations, as conditioning on the current state, future state, or a reward model as proposed by Janner et al. [27] can softly break the symmetry group as desired [7].

GATr-Diffuser is demonstrated on the problem of a Kuka robotic gripper stacking blocks using the “unconditional” environment introduced by Janner et al. [27]. We train a diffusion model based on a GATr denoising model on the offline trajectory dataset published with that paper. To facilitate a geometric interpretation, we parameterize the data in terms of geometric quantities like object positions and orientations. In particular, we use the position and pose of the robotic endeffector as features and map to joint angles with an inverse kinematics model. After training the diffusion model, it is integrated in a planning loop, closely following the setup (and using the code base) of Janner et al. [27]. It is then tested on its ability to stack four blocks on each other. We compare our GATr-Diffuser model to a reproduction of the original Diffuser model (based on the published code, but using our data parameterization) and a new transformer backbone for the Diffuser model. In addition, we show the published results of Diffuser [27], the equivariant EDGI [7], and the offline RL algorithms CQL [29] and BCQ [21] as published in Ref. [27]. The problem and hyperparameters are described in detail in Appendix C.

As shown in Tbl. 2 and Fig. 4, GATr-Diffuser solves the block-stacking problem better than all baselines. It is also clearly more sample-efficient, matching the performance of a Diffuser model or Transformer trained on the full dataset even when training only on 1% of the trajectories. The fact that GATr-Diffuser also outperforms the  $E(3)$ -equivariant EDGI model [7] is evidence that equivariance alone is not the key to its success, hinting that the geometric algebra provides a useful inductive bias.

## 5 Related work

**Geometric algebra** Geometric algebra (or Clifford algebra) was first conceived in the 19th century [10, 22] and has been used widely in quantum physics [15, 31]. Recently, it has found new popularity in computer graphics [17]. In particular, the projective geometric algebra used in this work [16, 32] and a conformal model [17] are suitable for 3D computations.

Geometric algebras have been used in machine learning in various ways. Spellings [40] use  $\mathbb{G}_{3,0,0}$  geometric products to compute rotation-invariant features from small point clouds. Unlike us, they do not learn internal geometric representations.

Method	Reward
GATr-Diffuser (ours)	<b>74.8 <math>\pm</math> 1.7</b>
Transformer-Diffuser	69.8 $\pm$ 1.9
Diffuser [27] (reproduced)	57.7 $\pm$ 1.8
Diffuser [27]	58.7 $\pm$ 2.5
EDGI [7]	62.0 $\pm$ 2.1
CQL [29]	24.4
BCQ [21]	0.0

Table 2: Diffusion-based robotic planning. We show the normalized cumulative rewards achieved on a robotic block stacking task [27], where 100 is optimal and means that each block stacking task is completed successfully, while 0 corresponds to a failure to stack any blocks. We show the mean and standard error over 200 evaluation episodes. The top three results were computed in the GATr code base, the bottom four taken from the literature [7, 27].

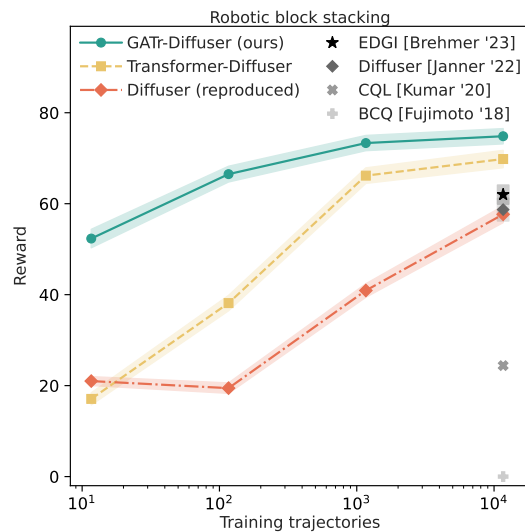


Figure 4: Diffusion-based robotic planning. We show normalized rewards (higher is better) as in Tbl. 2 as a function of training dataset size. GATr (—) is more successful at block stacking and more sample-efficient than the baselines, including the original Diffuser model [27] (—) and our modification of it based on a transformer (—). In grey, we show results reported by Brehmer et al. [7] and Janner et al. [27].

Our work was inspired by Brandstetter et al. [5] and Ruhe et al. [35]. These works also use multivector features (the latter even of the same  $\mathbb{G}_{3,0,1}$ ), and process them with operations such as the geometric / sandwich product, Clifford Fourier transforms and Clifford convolutions. The main difference to our work is that GATr is  $E(3)$  equivariant, while both of these works are not.<sup>12,13</sup>

**Equivariant deep learning** Equivariance to symmetries [11] is the primary design principle in modern geometric deep learning [8]. Equivariant networks have been applied successfully in areas such as medical imaging [30, 45] and robotics [26, 37, 43, 44, 47], and are ubiquitous in applications of machine learning to physics and chemistry [2, 3, 19]. The idea of using equivariant diffusion for robot motion planning was proposed by Brehmer et al. [7], where an equivariant U-Net was used.

In recent years, a number of works have investigated equivariant transformer and message-passing architectures [2, 3, 6, 19, 20, 33, 36]. These works are generally more limited in terms of the types of geometric quantities they can process, compared to our multivector features. Furthermore, our architecture is equivariant to the full group of Euclidean transformations, whereas previous works focus on  $SO(3)$ -equivariance.

**Diffusion models & transformers** Both transformers [42] and diffusion models [25, 38, 39] are at the core of several recent breakthroughs in language and image generation, and have a demonstrated ability to absorb large amounts of data. Recently, these models have also become popular in the context of reinforcement learning, where they can be used as policy or planner [9, 18, 27]. Our implementation of GATr into a diffusion model and planning algorithm fits into this line of work, closely following Janner et al. [27].

## 6 Discussion

We introduced the Geometric Algebra Transformer (GATr), a general-purpose architecture for geometric data. By representing data in projective geometric algebra, it provides a strong inductive bias conducive to representing various geometric interactions in three-dimensional space. GATr is  $E(3)$ -equivariant, guaranteeing a well-defined behaviour under transformations. Finally, GATr is based on the transformer architecture, inheriting its scalability, expressiveness, and versatility. To the best of our knowledge, GATr is the first  $E(3)$ -equivariant network based on learnable geometric algebra representations.

We demonstrated that the combination of geometric algebra and equivariance provides a strong inductive bias on  $n$ -body trajectory prediction and on a robotic manipulation benchmark. For the latter, we embedded GATr in a diffusion model to define an  $E(3)$ -invariant diffusion model. On both tasks, GATr outperformed multiple baselines, including vanilla transformers and an equivariant robotic planning method, in terms of peak performance, sample efficiency, and generalization.

One drawback of our approach is that since geometric algebra is not widely known yet, it may present an obstacle to understanding the details of the method. However, given a dictionary for embeddings of common objects and a library of primitives that act on them, *using* this framework is no more difficult than using typical neural network layers grounded in linear algebra. Another limitation of GATr in its current form is its computational efficiency. Although runtime is comparable to an unoptimized transformer implementation for the same hidden size, we do not (yet) have an optimized implementation with e. g. flash attention [14], and as always an equal-parameter comparison would lead to a larger hidden size for the equivariant model.

Optimizing the efficiency of the primitives on which GATr is built is thus one of the directions in which we plan further work. Another is the study of different design choices, such as the concrete geometric algebra or the symmetry group: does for instance the conformal geometric algebra  $\mathbb{G}_{4,1,0}$  offer benefits over  $\mathbb{G}_{3,0,1}$ ? Finally, the primitives we developed in this paper can be used to develop new architectures and algorithms, for instance geometric algebra-based equivariant message passing. Given the promising results presented in this work, we are looking forward to further study the potential of geometric algebra transformers in problems from molecular dynamics to robotics.

---

<sup>12</sup>Clifford convolutions are equivariant with respect to translations on a base space (similar to how regular convolutional networks are translation equivariant), but neither Brandstetter et al. [5], nor Ruhe et al. [35] are equivariant with respect to the  $E(3)$  symmetry naturally afforded by projective geometric algebra.

<sup>13</sup>Concurrently to this publication, Ref. [34] also studies equivariant, geometric algebra-based architectures.

**Acknowledgements** We would like to thank Joey Bose, Johannes Brandstetter, Gabriele Cesa, Steven De Keninck, Daniel Dijkman, Leo Dorst, Mario Geiger, and Evgeny Mironov for generous guidance regarding geometry, enthusiastic encouragement on equivariance, and careful counsel concerning computing complications.

## References

- [1] Alexei Baevski and Michael Auli. Adaptive input representations for neural language modeling. *arXiv preprint arXiv:1809.10853*, 2018.
- [2] Ilyes Batatia, David Peter Kovacs, Gregor N C Simm, Christoph Ortner, and Gabor Csanyi. MACE: Higher order equivariant message passing neural networks for fast and accurate force fields. In *Advances in Neural Information Processing Systems*, 2022.
- [3] Simon Batzner, Albert Musaelian, Lixin Sun, Mario Geiger, Jonathan P Mailoa, Mordechai Kornbluth, Nicola Molinari, Tess E Smidt, and Boris Kozinsky. E(3)-equivariant graph neural networks for data-efficient and accurate interatomic potentials. *Nat. Commun.*, 13(1):2453, May 2022.
- [4] Avishek Joey Bose and Ivan Kobyzev. Equivariant finite normalizing flows. *arXiv preprint arXiv:2110.08649*, 2021.
- [5] Johannes Brandstetter, Rianne van den Berg, Max Welling, and Jayesh K Gupta. Clifford neural layers for PDE modeling. *arXiv preprint arXiv:2209.04934*, 2022.
- [6] Johannes Brandstetter, Rob Hesselink, Elise van der Pol, Erik J Bekkers, and Max Welling. Geometric and physical quantities improve E(3) equivariant message passing. In *International Conference on Learning Representations*, 2022.
- [7] Johann Brehmer, Joey Bose, Pim De Haan, and Taco Cohen. EDGI: Equivariant Diffusion for Planning with Embodied Agents. *ICLR workshop on Reincarnating Reinforcement Learning*, 2023.
- [8] Michael M Bronstein, Joan Bruna, Taco Cohen, and Petar Veličković. Geometric deep learning: Grids, groups, graphs, geodesics, and gauges. 2021.
- [9] Lili Chen, Kevin Lu, Aravind Rajeswaran, Kimin Lee, Aditya Grover, Michael Laskin, Pieter Abbeel, Aravind Srinivas, and Igor Mordatch. Decision transformer: Reinforcement learning via sequence modeling. 2021.
- [10] William Kingdon Clifford. Applications of Grassmann’s Extensive Algebra. *Amer. J. Math.*, 1(4):350–358, 1878.
- [11] Taco Cohen. *Equivariant Convolutional Networks*. PhD thesis, University of Amsterdam, 2021.
- [12] Taco Cohen and Max Welling. Group equivariant convolutional networks. In *International conference on machine learning*, pages 2990–2999. PMLR, 2016.
- [13] Erwin Coumans and Yunfei Bai. PyBullet, a Python module for physics simulation for games, robotics and machine learning. <http://pybullet.org>, 2016–2019.
- [14] Tri Dao, Dan Fu, Stefano Ermon, Atri Rudra, and Christopher Ré. FlashAttention: Fast and memory-efficient exact attention with IO-awareness. *Advances in Neural Information Processing Systems*, 35:16344–16359, 2022.
- [15] C Doran and A Lasenby. *Geometric algebra for physicists*. Cambridge University Press, 2003.
- [16] Leo Dorst. A guided tour to the plane-based geometric algebra pga. 2020. URL <https://geometricalgebra.org/downloads/PGA4CS.pdf>.
- [17] Leo Dorst, Daniel Fontijne, and Stephen Mann. *Geometric Algebra for Computer Science: An Object-oriented Approach to Geometry*. Morgan Kaufmann Series in Computer Graphics. Morgan Kaufmann, Amsterdam, 2007. ISBN 978-0-12-369465-2.

- [18] Scott Emmons, Benjamin Eysenbach, Ilya Kostrikov, and Sergey Levine. RvS: What is essential for offline RL via supervised learning? 2022.
- [19] Thorben Frank, Oliver Thorsten Unke, and Klaus Robert Muller. So3krates: Equivariant attention for interactions on arbitrary length-scales in molecular systems. October 2022.
- [20] Fabian B Fuchs, Daniel E Worrall, Volker Fischer, and Max Welling. SE(3)-Transformers: 3D Roto-Translation equivariant attention networks. In *Advances in Neural Information Processing Systems*, 2020.
- [21] Scott Fujimoto, David Meger, and Doina Precup. Off-policy deep reinforcement learning without exploration. In *International conference on machine learning*, pages 2052–2062. PMLR, 2019.
- [22] Hermann Grassmann. *Die lineale Ausdehnungslehre*. Otto Wigand, Leipzig, 1844.
- [23] Dan Hendrycks and Kevin Gimpel. Gaussian error linear units (gelus). *arXiv preprint arXiv:1606.08415*, 2016.
- [24] Jonathan Ho, Nal Kalchbrenner, Dirk Weissenborn, and Tim Salimans. Axial attention in multidimensional transformers. *arXiv:1912.12180 [cs]*, December 2019.
- [25] Jonathan Ho, Ajay Jain, and Pieter Abbeel. Denoising diffusion probabilistic models. In *Neural Information Processing Systems*, 2020.
- [26] Haojie Huang, Dian Wang, Robin Walters, and Robert Platt. Equivariant transporter network. In *Proceedings of Robotics: Science and Systems*, 2022.
- [27] Michael Janner, Yilun Du, Joshua Tenenbaum, and Sergey Levine. Planning with diffusion for flexible behavior synthesis. In *International Conference on Machine Learning*, 2022.
- [28] Jonas Köhler, Leon Klein, and Frank Noé. Equivariant flows: exact likelihood generative learning for symmetric densities. In *International conference on machine learning*, pages 5361–5370. PMLR, 2020.
- [29] Aviral Kumar, Aurick Zhou, George Tucker, and Sergey Levine. Conservative q-learning for offline reinforcement learning. *Advances in Neural Information Processing Systems*, 33: 1179–1191, 2020.
- [30] Maxime W Lafarge, Erik J Bekkers, Josien P W Pluim, Remco Duits, and Mitko Veta. Roto-translation equivariant convolutional networks: Application to histopathology image analysis. *Med. Image Anal.*, 68, 2021.
- [31] Pertti Lounesto. *Clifford Algebras and Spinors*. London Mathematical Society Lecture Note. Cambridge University Press, 2001.
- [32] Martin Roelfs and Steven De Keninck. Graded symmetry groups: plane and simple. *arXiv preprint arXiv:2107.03771*, 2021.
- [33] David W Romero, Erik J Bekkers, Jakub M Tomczak, and Mark Hoogendoorn. Attentive group equivariant convolutional networks. In *Proceedings of the 37th International Conference on Machine Learning*, volume 119, pages 8188–8199. JMLR.org, July 2020.
- [34] David Ruhe, Johannes Brandstetter, and Patrick Forré. Clifford group equivariant neural networks. *arXiv preprint arXiv:2305.11141*, 2023.
- [35] David Ruhe, Jayesh K Gupta, Steven de Keninck, Max Welling, and Johannes Brandstetter. Geometric clifford algebra networks. *arXiv preprint arXiv:2302.06594*, 2023.
- [36] Víctor Garcia Satorras, Emiel Hoogeboom, and Max Welling. E(n) equivariant graph neural networks. In Marina Meila and Tong Zhang, editors, *Proceedings of the 38th International Conference on Machine Learning*, volume 139 of *Proceedings of Machine Learning Research*, pages 9323–9332. PMLR, 2021.

- [37] Anthony Simeonov, Yilun Du, Andrea Tagliasacchi, Joshua B Tenenbaum, Alberto Rodriguez, Pulkit Agrawal, and Vincent Sitzmann. Neural descriptor fields: SE(3)-Equivariant object representations for manipulation. In *ICRA*, 2022.
- [38] Jascha Sohl-Dickstein, Eric Weiss, Niru Maheswaranathan, and Surya Ganguli. Deep unsupervised learning using nonequilibrium thermodynamics. In *International Conference on Machine Learning*, pages 2256–2265. PMLR, 2015.
- [39] Yang Song and Stefano Ermon. Generative modeling by estimating gradients of the data distribution. *Adv. Neural Inf. Process. Syst.*, 32, 2019.
- [40] Matthew Spellings. Geometric algebra attention networks for small point clouds. *arXiv preprint arXiv:2110.02393*, 2021.
- [41] Jianlin Su, Yu Lu, Shengfeng Pan, Bo Wen, and Yunfeng Liu. Roformer: Enhanced transformer with rotary position embedding. *arXiv preprint arXiv:2104.09864*, 2021.
- [42] Ashish Vaswani, Noam Shazeer, Niki Parmar, Jakob Uszkoreit, Llion Jones, Aidan N Gomez, Łukasz Kaiser, and Illia Polosukhin. Attention is all you need. In *Advances in Neural Information Processing Systems*, volume 30, 2017.
- [43] Dian Wang, Robin Walters, Xupeng Zhu, and Robert Platt. Equivariant Q learning in spatial action spaces, 2021.
- [44] Dian Wang, Mingxi Jia, Xupeng Zhu, Robin Walters, and Robert Platt. On-Robot learning with equivariant models. In *CoRL*, 2022.
- [45] Marysia Winkels and Taco Cohen. Pulmonary nodule detection in CT scans with equivariant CNNs. *MIA*, 2019.
- [46] Ruibin Xiong, Yunchang Yang, Di He, Kai Zheng, Shuxin Zheng, Chen Xing, Huishuai Zhang, Yanyan Lan, Liwei Wang, and Tieyan Liu. On layer normalization in the transformer architecture. In *International Conference on Machine Learning*, pages 10524–10533. PMLR, 2020.
- [47] Xupeng Zhu, Dian Wang, Ondrej Biza, Guanang Su, Robin Walters, and Robert Platt. Sample efficient grasp learning using equivariant models. In *Robotics: Science and Systems XVIII*. Robotics: Science and Systems Foundation, June 2022.

## A Theoretical results

In this section, we state or prove several properties of equivariant maps between geometric algebras that we use in the construction of GATr.

The grade involution is a linear involutive bijection  $\widehat{\cdot} : \mathbb{G}_{n,0,r} \rightarrow \mathbb{G}_{n,0,r}$ , which sends a  $k$ -blade  $x$  to  $\widehat{x} = (-1)^k x$ . Note that this is an algebra automorphism  $\widehat{xy} = \widehat{x}\widehat{y}$ , and also an  $\wedge$ -algebra automorphism. The reversal in a linear involutive bijection  $\widetilde{\cdot} : \mathbb{G}_{n,0,r} \rightarrow \mathbb{G}_{n,0,r}$  which sends a  $k$ -blade  $x = x_1 \wedge x_2 \wedge \dots \wedge x_k$  to the reverse:  $\widetilde{x} = x_k \wedge \dots \wedge x_2 \wedge x_1 = \pm x$  with  $+x$  if  $k \in \{0, 1, 4, 5, \dots, 8, 9, \dots\}$  and  $-x$  otherwise. Note that this is an anti-automorphism (contravariant functor):  $\widetilde{xy} = \widetilde{y}\widetilde{x}$ .

Here we denote the sandwich action of  $u \in \text{Pin}(n, 0, r)$  on a multivector  $x$  not as  $\rho_u(x)$ , but as  $u[x]$ . For odd  $u$ ,  $u[x] = u\widehat{x}u^{-1}$ , while for even  $u$ ,  $u[x] = uxu^{-1}$ . The sandwich action is linear by linearity of the  $\widehat{\cdot}$  and bilinearity of the geometric product. Furthermore, note that for any particular  $u \in \text{Pin}(n, 0, r)$ , the action is a geometric algebra homomorphism:  $u[ab] = u\widehat{ab}u^{-1} = u\widehat{a}u^{-1}u\widehat{b}u^{-1} = u[a]u[b]$ . By linearity and a symmetrization argument [17, Sec 7.1], one can show that it also a  $\wedge$ -algebra homomorphism (outermorphism):  $u[a \wedge b] = u[a] \wedge u[b]$ .

Let  $l \geq k$ . Given a  $k$ -vector  $a$  and  $l$ -vector  $b$ , define the *left contraction* as  $a|b := \langle ab \rangle_{l-k}$ , which is a  $l-k$ -vector. For  $k = 1$ , and  $b$  a blade  $b = b_1 \wedge \dots \wedge b_l$ . Geometrically,  $a|b$  is the projection of  $a$  to the space spanned by the vectors  $b_i$ . Thus we have that  $a|b = 0 \iff \forall i, \langle a, b_i \rangle = 0$  [17, Sec 3.2.3], in which case we define  $a$  and  $b$  to be *orthogonal*. In particular, two vectors  $a, b$  are orthogonal if their inner product is zero. Furthermore, we define a vector  $a$  to be *tangential* to blade  $b$  if  $a \wedge b = 0$ .

In the projective algebra, a blade  $x$  is defined to be *ideal* if it can be written as  $x = e_0 \wedge y$  for another blade  $y$ .

### A.1 Linear maps

We begin with  $\text{Pin}$ -equivariant linear maps. After some technical lemmata, we prove the most general form of linear equivariant maps in the Euclidean geometric algebra  $\mathbb{G}_{n,0,0}$ , and then also in projective geometric algebra  $\mathbb{G}_{n,0,1}$ .

**Proposition 2.** *The grade projection  $\langle \cdot \rangle_k$  is equivariant [17, Sec 13.2.3].*

*Proof.* Choose an  $l$ -blade  $x = a_1 \wedge a_2 \wedge \dots \wedge a_l$ . Let  $u$  be a 1-versor. As the action  $u$  is an outermorphism,  $u[x] = u[a_1] \wedge \dots \wedge u[a_l]$  is an  $l$ -blade. Now if  $l \neq k$ , then  $\langle x \rangle_k = 0$  and thus  $u[\langle x \rangle_k] = \langle u[x] \rangle_k$ . If  $l = k$ , then  $\langle x \rangle_k = x$  and thus  $u[\langle x \rangle_k] = \langle u[x] \rangle_k$ . As the grade projection is linear, equivariance extends to any multivector.  $\square$

**Proposition 3.** *The following map is equivariant:  $\phi : \mathbb{G}_{3,0,1} \rightarrow \mathbb{G}_{3,0,1} : x \mapsto e_0 x$ .*

*Proof.* Let  $u$  be a 1-versor, then  $u$  acts on a multivector as  $x \mapsto u[x] = u\widehat{x}u^{-1}$ , where  $\widehat{x}$  is the grade involution. Note that  $e_0$  is invariant:  $u[e_0] = -ue_0u^{-1} = e_0uu^{-1} = e_0$ , where  $ue_0 = -e_0u$  because  $u$  and  $e_0$  are orthogonal:  $ue_0 = \langle u, e_0 \rangle + u \wedge e_0 = -e_0 \wedge u = -e_0 \wedge u$ . Then  $\phi$  is equivariant, as the action is an algebra homomorphism:  $u[\phi(x)] = u[e_0x] = ue_0\widehat{x}u^{-1} = ue_0u^{-1}u\widehat{x}u^{-1} = ue_0u[x] = e_0u[x] = \phi(u[x])$ . It follows that  $\phi$  is also equivariant to any product of vectors, i.e. any versor  $u$ .  $\square$

**Euclidean geometric algebra** Before constructing the most general equivariant linear map between multivectors in projective geometric algebra, we begin with the Euclidean case  $\mathbb{G}_{n,0,0}$ .

**Theorem 1** (Cartan-Dieuodonné). *Every orthogonal transformation of an  $n$ -dimensional space can be decomposed into at most  $n$  reflections in hyperplanes.*

*Proof.* This theorem is proven in Roelfs and De Keninck [32].  $\square$

**Lemma 1.** *In the  $n$ -dimensional Euclidean geometric algebra  $\mathbb{G}_{n,0,0}$ , the group  $\text{Pin}(n, 0, 0)$  acts transitively on the space of  $k$ -blades of norm  $\lambda \in \mathbb{R}^{>0}$ .*

*Proof.* As the Pin group preserves norm, choose  $\lambda = 1$  without loss of generality. Any  $k$ -blade  $x$  of unit norm can be written by Gram-Schmidt factorization as the wedge product of  $k$  orthogonal vectors of unit norm  $x = v_1 \wedge v_2 \wedge \dots \wedge v_k$ . Consider another  $k$ -blade  $y = w_1 \wedge w_2 \wedge \dots \wedge w_k$  with  $w_i$  orthonormal. We'll construct a  $u \in \text{Pin}(n, 0, 0)$  such that  $u[x] = y$ .

Choose  $n - k$  additional orthonormal vectors  $v_{k+1}, \dots, v_n$  and  $w_{k+1}, \dots, w_n$  to form orthonormal bases. Then, there exists a unique orthogonal transformation  $\mathbb{R}^n \rightarrow \mathbb{R}^n$  that maps  $v_i$  into  $w_i$  for all  $i \in \{1, \dots, n\}$ . By the Cartan-Dieudonné theorem 1, this orthogonal transformation can be expressed as the product of reflections, thus there exists a  $u \in \text{Pin}(n, 0, 0)$  such that  $u[v_i] = w_i$ . As the  $u$  action is a  $\wedge$ -algebra homomorphism ( $u[a \wedge b] = u[a] \wedge u[b]$ , for any multivectors  $a, b$ ), we have that  $u[x] = y$ .  $\square$

**Lemma 2.** *In the Euclidean ( $r = 0$ ) or projective ( $r = 1$ ) geometric algebra  $\mathbb{G}_{n,0,r}$ , let  $x$  be a  $k$ -blade. Let  $u$  be a 1-vensor. Then  $u[x] = x \iff u \lrcorner x = 0$  and  $u[x] = -x \iff u \wedge x = 0$ .*

*Proof.* Let  $x$  be a  $k$ -blade and  $u$  a vector of unit norm. We can decompose  $u$  into  $u = t + v$  with  $t \wedge x = 0$  (the part tangential to the subspace of  $x$ ) and  $v \lrcorner x = 0$  (the normal part). This decomposition is unique unless  $x$  is ideal in the projective GA, in which case the  $e_0$  component of  $u$  is both normal and tangential, and we choose  $t$  Euclidean.

In either case, note the following equalities:  $xt = (-1)^{k-1}tx$ ;  $xv = (-1)^k vx$ ;  $vt = -tv$  and note  $\nexists \lambda \neq 0$  such that  $vtx = \lambda x$ , which can be shown e.g. by picking a basis. Then:

$$u[x] = (-1)^k(t + v)x(t + v) = (t + v)(-t + v)x = (-\|t\|^2 + \|v\|^2)x - 2vtx$$

We have  $u[x] \propto x \iff vtx = 0$ . If  $x$  is not ideal, this implies that either  $v = 0$  (thus  $u \wedge x = 0$  and  $u[x] = -x$ ) or  $t = 0$  (thus  $u \lrcorner x = 0$  and  $u[x] = x$ ). If  $x$  is ideal, this implies that either  $v \propto e_0$  (thus  $u \wedge x = 0$  and  $u[x] = -x$ ) or  $t = 0$  (thus  $u \lrcorner x = 0$  and  $u[x] = x$ ).  $\square$

**Lemma 3.** *Let  $r \in \{0, 1\}$ . Any linear  $\text{Pin}(n, 0, r)$ -equivariant map  $\phi : \mathbb{G}_{n,0,r} \rightarrow \mathbb{G}_{n,0,r}$  can be decomposed into a sum of equivariant maps  $\phi = \sum_{lkm} \phi_{lkm}$ , with  $\phi_{lkm}$  equivariantly mapping  $k$ -blades to  $l$ -blades. If  $r = 0$  (Euclidean algebra) or  $k < n + 1$ , such a map  $\phi_{lkm}$  is defined by the image of any one non-ideal  $k$ -blade, like  $e_{12\dots k}$ . Instead, if  $r = 1$  (projective algebra) and  $k = n + 1$ , then such a map is defined by the image of a pseudoscalar, like  $e_{01\dots n}$ .*

*Proof.* The  $\text{Pin}(n, 0, r)$  group action maps  $k$ -vectors to  $k$ -vectors. Therefore,  $\phi$  can be decomposed into equivariant maps from grade  $k$  to grade  $l$ :  $\phi(x) = \sum_{lk} \phi_{lk}(\langle x \rangle_k)$ , with  $\phi_{lk}$  having  $l$ -vectors as image, and all  $k'$ -vectors in the kernel, for  $k' \neq k$ . Let  $x$  be an non-ideal  $k$ -blade (or pseudoscalar if  $k = n + 1$ ). By lemmas 1 and 4, in both Euclidean and projective GA, the span of the  $k$ -vectors in the orbit of  $x$  contains any  $k$ -vector. So  $\phi_{lk}$  is defined by the  $l$ -vector  $y = \phi_{lk}(x)$ . Any  $l$ -vector can be decomposed as a finite sum of  $l$ -blades:  $y = y_1 + \dots + y_M$ . We can define  $\phi_{lkm}(x) = y_m$ , extended to all  $l$ -vectors by equivariance, and note that  $\phi_{lk} = \sum_m \phi_{lkm}$ .  $\square$

**Proposition 4.** *For an  $n$ -dimensional Euclidean geometric algebra  $\mathbb{G}_{n,0,0}$ , any linear endomorphism  $\phi : \mathbb{G}_{n,0,0} \rightarrow \mathbb{G}_{n,0,0}$  that is equivariant to the  $\text{Pin}(n, 0, 0)$  group (equivalently to  $O(n)$ ) is of the type  $\phi(x) = \sum_{k=0}^n w_k \langle x \rangle_k$ , for parameters  $w \in \mathbb{R}^{n+1}$ .*

*Proof.* By decomposition of Lemma 3, let  $\phi$  map from  $k$ -blades to  $l$ -blades. Let  $x$  be a  $k$ -blade. Let  $u$  be a 1-vensor. By Lemma 2, if  $u$  is orthogonal to  $x$ ,  $u[\phi(x)] = \phi(u[x]) = \phi(x)$  and  $u$  is also orthogonal to  $\phi(x)$ . If  $u \wedge x = 0$ , then  $u[\phi(x)] = \phi(u[x]) = \phi(-x) = -\phi(x)$  and  $u \wedge \phi(x) = 0$ . Thus any vector in  $x$  is in  $\phi(x)$  and any vector orthogonal to  $x$  is orthogonal to  $\phi(x)$ , this implies  $\phi(x) = w_k x$ , for some  $w_k \in \mathbb{R}$ . By Lemma 3, we can extend  $\phi$  to  $\phi(y) = w_k y$  for any  $k$ -vector  $y$ .  $\square$

**Projective geometric algebra** How about equivariant linear maps in *projective* geometric algebra? The degenerate metric makes the derivation more involved, but in the end we will arrive at a result that is only slightly more general.

**Lemma 4.** *The Pin group of the projective geometric algebra,  $\text{Pin}(n, 0, 1)$ , acts transitively on the space of  $k$ -blades with positive norm  $\|x\| = \lambda > 0$ . Additionally, the group acts transitively on the space of zero-norm  $k$ -blades of the form  $x = e_0 \wedge y$  (called ideal blades), with  $\|y\| = \kappa$ .*

*Proof.* Let  $x = x_1 \wedge \dots \wedge x_k$  be a  $k$ -blade with positive norm  $\lambda$ . All vectors  $x_i$  can be written as  $x_i = v_i + \delta_i e_0$ , for a nonzero Euclidean vector  $v_i$  (meaning with no  $e_0$  component) and  $\delta_i \in \mathbb{R}$ , because if  $v_i = 0$ , the norm of  $x$  would have been 0. Orthogonalize them as  $x'_2 = x_2 - \langle x_1, x_2 \rangle x_1$ , etc., resulting in  $x = x'_1 \wedge \dots \wedge x'_k$  with  $x'_i = v'_i + \delta'_i e_0$  with orthogonal  $v'_i$ .

Define the translation  $t = 1 + \frac{1}{2} \sum_i \delta'_i e_0 \wedge v'_i$ , which makes  $x'$  Euclidean:  $t[x'] = v'_1 \wedge \dots \wedge v'_k$ . By Lemma 1, the Euclidean Pin group  $\text{Pin}(n, 0, 0)$ , which is a subgroup of  $\text{Pin}(n, 0, 1)$ , acts transitively on Euclidean  $k$ -blades of a given norm. Thus, in the projective geometric algebra  $\text{Pin}(n, 0, 1)$ , any two  $k$ -blades of equal positive norm  $\lambda$  are related by a translation to the origin and then a  $\text{Pin}(n, 0, 0)$  transformation.

For the ideal blades, let  $x = e_0 \wedge y$ , with  $\|y\| = \kappa$ . We take  $y$  to be Euclidean without loss of generality. For any  $g \in \text{Pin}(n, 0, 1)$ ,  $g[e_0] = e_0$ , so  $g[x] = e_0 \wedge g[y]$ . Consider another  $x' = e_0 \wedge y'$  with  $\|y'\| = \kappa$  and taking  $y'$  Euclidean. As  $\text{Pin}(n, 0, 0)$  acts transitively on Euclidean  $(k-1)$ -blades with norm  $\kappa$ , let  $g \in \text{Pin}(n, 0, 0)$  such that  $g[y] = y'$ . Then  $g[x] = x'$ .  $\square$

We can now construct the most general equivariant linear map between projective geometric algebras, a key ingredient for GATr:

**Proposition 5.** *For the projective geometric algebra  $\mathbb{G}_{n,0,1}$ , any linear endomorphism  $\phi : \mathbb{G}_{n,0,1} \rightarrow \mathbb{G}_{n,0,1}$  that is equivariant to the group  $\text{Pin}(n, 0, r)$  (equivalently to  $E(n)$ ) is of the type  $\phi(x) = \sum_{k=0}^{n+1} w_k \langle x \rangle_k + \sum_{k=0}^n v_k e_0 \langle x \rangle_k$ , for parameters  $w \in \mathbb{R}^{n+2}$ ,  $v \in \mathbb{R}^{n+1}$ .*

*Proof.* Following Lemma 3, decompose  $\phi$  into a linear equivariant map from  $k$ -blades to  $l$ -blades. For  $k < n+1$ , let  $x = e_{12\dots k}$ . Then following Lemma 2, for any  $1 \leq i \leq k$ ,  $e_i \wedge x = 0$ ,  $e_i[x] = -x$ , and  $e_i[\phi(x)] = \phi(e_i[x]) = \phi(-x) = -\phi(x)$  and thus  $e_i \wedge \phi(x) = 0$ . Therefore, we can write  $\phi(x) = x \wedge y_1 \wedge \dots \wedge y_{l-k}$ , for  $l-k$  vectors  $y_j$  orthogonal to  $x$ .

Also, again using Lemma 2, for  $k < i \leq n$ ,  $e_i[x] = 0 \implies e_i[\phi(x)] = \phi(x) \implies e_i[\phi(x)] = 0 \implies \forall i, \langle e_i, y_j \rangle = 0$ . Thus,  $y_j$  is orthogonal to all  $e_i$  with  $1 \leq i \leq n$ . Hence,  $l = k$  or  $l = k+1$  and  $y_1 \propto e_0$ .

For  $k = n+1$ , let  $x = e_{012\dots k}$ . By a similar argument, all invertible vectors  $u$  tangent to  $x$  must be tangent to  $\phi(x)$ , thus we find that  $\phi(x) = x \wedge y$  for some blade  $y$ . For any non-zero  $\phi(x)$ ,  $y \propto 1$ , and thus  $\phi(x) \propto x$ . By Lemma 3, by equivariance and linearity, this fully defines  $\phi$ .  $\square$

## A.2 Bilinear maps

Next, we turn towards bilinear operations. In particular, we show that the geometric product and the join are equivariant.

For the geometric product, equivariance is straightforward: Any transformation  $u \in \text{Pin}(n, 0, r)$ , gives a homomorphism of the geometric algebra, as for any multivectors  $x, y$ ,  $u[xy] = uxyu^{-1} = u\hat{x}\hat{y}u^{-1} = u\hat{x}u^{-1}u\hat{y}u^{-1} = u[x]u[y]$ . The geometric product is thus equivariant.

**Dual and join in Euclidean algebra** For the join and the closely related dual, we again begin with the Euclidean geometric algebra, before turning to the projective case later.

The role of the dual is to have a bijection  $\cdot^* : \mathbb{G}_{n,0,0} \rightarrow \mathbb{G}_{n,0,0}$  that maps  $k$ -vectors to  $(n-k)$ -vectors. For the Euclidean algebra, with a choice of pseudoscalar  $\mathcal{I}$ , we can define a dual as:

$$x^* = x\mathcal{I}^{-1} = x\tilde{\mathcal{I}} \tag{6}$$

This dual is bijective, and involutive up to a sign:  $(y^*)^* = y\tilde{\mathcal{I}}\tilde{\mathcal{I}} = \pm y$ , with  $+y = 1$  for  $n \in \{1, 4, 5, 8, 9, \dots\}$  and  $-y$  for  $n \in \{2, 3, 6, 7, \dots\}$ . We choose  $\tilde{\mathcal{I}}$  instead of  $\mathcal{I}$  in the definition of the dual so that given  $n$  vectors  $x_1, \dots, x_n$ , the dual of the multivector  $x = x_1 \wedge \dots \wedge x_n$ , is given by the scalar of the oriented volume spanned by the vector. We denote the inverse of the dual as  $x^{-*} = x\mathcal{I}$ . Expressed in a basis, the dual yields the complementary indices and a sign. For example, for  $n = 3$  and  $\mathcal{I} = e_{123}$ , we have  $(e_1)^* = -e_{23}$ ,  $(e_{12})^* = e_3$ .

Via the dual, we can define the bilinear join operation, for multivectors  $x, y$ :

$$x \vee y := (x^* \wedge y^*)^{-*} = ((x\tilde{\mathcal{I}}) \wedge (y\tilde{\mathcal{I}}))\mathcal{I}.$$

**Lemma 5.** *In Euclidean algebra  $\mathbb{G}_{n,0,0}$ , the join is  $\text{Spin}(n, 0, 0)$  equivariant. Furthermore, it is  $\text{Pin}(n, 0, 0)$  equivariant if and only if  $n$  is even.*

*Proof.* The join is equivariant to the transformations from the group  $\text{Spin}(n, 0, 0)$ , which consists of the product of an even amount of unit vectors, because such transformations leave the pseudoscalar  $\mathcal{I}$  invariant, and the operation consists otherwise of equivariant geometric and wedge products.

However, let  $e_{12\dots n} = \mathcal{I} \in \text{Pin}(n, 0, 0)$  be the point reflection, which negates vectors of odd grades by the grade involution:  $\mathcal{I}[x] = \hat{x}$ . Let  $x$  be a  $k$ -vector and  $y$  an  $l$ -vector. Then  $x \vee y$  is a vector of grade  $n - ((n - k) + (n - l)) = k + l - n$  (and zero if  $k + l < n$ ). Given that the join is bilinear, the inputs transform as  $(-1)^{k+l}$  under the point reflection, while the transformed output gets a sign  $(-1)^{k+l-n}$ . Thus for odd  $n$ , the join is not  $\text{Pin}(n, 0, 0)$  equivariant.  $\square$

To address this, given a pseudoscalar  $z = \lambda \mathcal{I}$ , we can create an equivariant Euclidean join via:

$$\text{EquiJoin}(x, y, z = \lambda \mathcal{I}) := \lambda(x \vee y) = \lambda(x^* \wedge y^*)^{-*}. \quad (7)$$

**Proposition 6.** *In Euclidean algebra  $\mathbb{G}_{n,0,0}$ , the equivariant join  $\text{EquiJoin}$  is  $\text{Pin}(n, 0, 0)$  equivariant.*

*Proof.* The  $\text{EquiJoin}$  is a multilinear operation, so for  $k$ -vector  $x$  and  $l$ -vector  $y$ , under a point reflection, the input gets a sign  $(-1)^{k+l+n}$  while the output is still a  $k + l - n$  vector and gets sign  $(-1)^{k+l-n}$ . These signs differ by even  $(-1)^{2n} = 1$  and thus  $\text{EquiJoin}$  is  $\text{Pin}(n, 0, 1)$ -equivariant.  $\square$

We prove two equalities of the Euclidean join which we use later.

**Lemma 6.** *In the algebra  $\mathbb{G}_{n,0,0}$ , let  $v$  be a vector and  $x, y$  be multivectors. Then*

$$v \rfloor (x \vee y) = (v \rfloor x) \vee y \quad (8)$$

and

$$x \vee (v \rfloor y) = -(-1)^n \widehat{v \rfloor x} \vee y. \quad (9)$$

*Proof.* For the first statement, let  $a$  be a  $k$ -vector and  $b$  an  $l$ -vector. Then note the following two identities:

$$\begin{aligned} a \vee b &= \langle a^* b \tilde{\mathcal{I}} \rangle_{2n-k-l} \mathcal{I} = \langle a^* b \rangle_{n-(2n-k-l)} \tilde{\mathcal{I}} \mathcal{I} = \langle a^* b \rangle_{k+l-n} = a^* \rfloor b, \\ (v \rfloor a)^* &= \langle v a \rangle_{k-1} \tilde{\mathcal{I}} = \langle v a \tilde{\mathcal{I}} \rangle_{n-k+1} = \langle v a^* \rangle_{n-k+1} = v \rfloor (a^*). \end{aligned}$$

Combining these and the associativity of  $\rfloor$  gives:

$$(v \rfloor a) \vee b = (v \rfloor a)^* \rfloor b = v \rfloor (a^*) \rfloor b = v \rfloor (a \vee b)$$

For the second statement, swapping  $k$ -vector  $a$  and  $l$ -vector  $b$  incurs  $a \vee b = (a^* \wedge b^*)^{-*} = (-1)^{(n-k)(n-l)} (b^* \wedge a^*)^{-*} = (-1)^{(n-k)(n-l)} (b \vee a)$ . Then we get:

$$\begin{aligned} a \vee (v \rfloor b) &= (-1)^{(n-k)(n-l-1)} (v \rfloor b) \vee a \\ &= (-1)^{(n-k)(n-l-1)} v \rfloor (b \vee a) \\ &= (-1)^{(n-k)(n-l-1)+(n-k)(n-l)} v \rfloor (a \vee b) \\ &= (-1)^{(n-k)(n-l-1)+(n-k)(n-l)} (v \rfloor a) \vee b \\ &= (-1)^{(n-k)(2n-2l-1)} (v \rfloor a) \vee b \\ &= (-1)^{k-n} (v \rfloor a) \vee b \\ &= -(-1)^{k-1-n} (v \rfloor a) \vee b \\ &= -(-1)^n \widehat{(v \rfloor a)} \vee b. \end{aligned}$$

This generalizes to multivectors  $x, y$  by linearity.  $\square$

**Dual and join in projective algebra** For the projective algebra  $\mathbb{G}_{n,0,1}$  with its degenerate inner product, the dual definition of Eq. 6 unfortunately does not yield a bijective dual. For example,  $\widetilde{e_0 e_{012\dots n}} = 0$ . For a bijective dual that yields the complementary indices on basis elements, a different definition is needed. Following Dorst [16], we use the right complement. This involves choosing an orthogonal basis and then for a basis  $k$ -vector  $x$  to define the dual  $x^*$  to be the basis  $n+1-k$ -vector such that  $x \wedge x^* = \mathcal{I}$ , for pseudoscalar  $\mathcal{I} = e_{012\dots n}$ . For example, this gives dual  $e_{01}^* = e_{23}$ , so that  $e_{01} \wedge e_{23} = e_{0123}$ .

This dual is still easy to compute numerically, but it can no longer be constructed solely from operations available to us in the geometric algebra. This makes it more difficult to reason about equivariance.

**Proposition 7.** *In the algebra  $\mathbb{G}_{n,0,1}$ , the join  $a \vee b = (a^* \wedge b^*)^{-*}$  is equivariant to  $\text{Spin}(n, 0, 1)$ .*

*Proof.* Even though the dual is not a  $\mathbb{G}_{n,0,1}$  operation, we can express the join in the algebra as follows. We decompose a  $k$ -vector  $x$  as  $x = t_x + e_0 p_x$  into a Euclidean  $k$ -vector  $t_x$  and a Euclidean  $(k-1)$ -vector  $p_x$ . Then Dorst [16, Eq (35)] computes the following expression

$$\begin{aligned} (t_x + e_0 p_x) \vee (t_y + e_0 p_y) &= ((t_x + e_0 p_x)^* \wedge (t_y + e_0 p_y)^*)^{-*} \\ &= t_x \vee_{\text{Euc}} p_y + (-1)^n \widehat{p_x} \vee_{\text{Euc}} t_y + e_0 (p_x \vee_{\text{Euc}} p_y), \end{aligned} \quad (10)$$

where the Euclidean join of vectors  $a, b$  in the projective algebra is defined to equal the join of the corresponding vectors in the Euclidean algebra:

$$a \vee_{\text{Euc}} b := ((a \widetilde{e_{12\dots n}}) \wedge (b \widetilde{e_{12\dots n}})) e_{12\dots n}$$

The operation  $a \vee_{\text{Euc}} b$  is  $\text{Spin}(n, 0, 0)$  equivariant, as discussed in Lemma 5. For any rotation  $r \in \text{Spin}(n, 0, 1)$  (which is Euclidean), we thus have  $r[a \vee_{\text{Euc}} b] = r[a] \vee_{\text{Euc}} r[b]$ . This makes the PGA dual in Eq. (10) equivariant to the rotational subgroup  $\text{Spin}(n, 0, 0) \subset \text{Spin}(n, 0, 1)$ .

We also need to show equivariance to translations. Let  $v$  be a Euclidean vector and  $\tau = 1 - e_0 v/2$  a translation. Translations act by shifting with  $e_0$  times a contraction:  $\tau[x] = x - e_0(v \rfloor x)$ . This acts on the decomposed  $x$  in the following way:  $\tau[t_x + e_0 p_x] = \tau[t_x] + e_0 p_x = t_x + e_0(p_x - v \rfloor t_x)$ .

We thus get:

$$\begin{aligned} \tau[x] \vee \tau[y] &= (\tau[t_x] + e_0 p_x) \vee (\tau[t_y] + e_0 p_y) \\ &= (t_x + e_0(p_x - v \rfloor t)) \vee (t_y + e_0(p_y - v \rfloor t_y)) \\ &= x \vee y - t_x \vee_{\text{Euc}} (v \rfloor t_y) - (-1)^n v \rfloor t_x \vee_{\text{Euc}} t_y \\ &\quad - e_0(p_x \vee_{\text{Euc}} (v \rfloor t_y) + (v \rfloor t_x) \vee_{\text{Euc}} p_y) \quad \text{Used (10) \& linearity} \\ &= x \vee y - e_0(p_x \vee_{\text{Euc}} (v \rfloor t_y) + (v \rfloor t_x) \vee_{\text{Euc}} p_y) \quad \text{Used (9)} \\ &= x \vee y - e_0 \left( -(-1)^n v \rfloor \widehat{p_x} \vee_{\text{Euc}} t_y + (v \rfloor t_x) \vee_{\text{Euc}} p_y \right) \quad \text{Used (9)} \\ &= x \vee y - e_0 \left( (-1)^n (v \rfloor \widehat{p_x}) \vee_{\text{Euc}} t_y + (v \rfloor t_x) \vee_{\text{Euc}} p_y \right) \\ &= x \vee y - e_0(v \rfloor \{(-1)^n \widehat{p_x} \vee_{\text{Euc}} t_y + t_x \vee_{\text{Euc}} p_y\}) \quad \text{Used (8)} \\ &= \tau[x \vee y] \end{aligned}$$

The join is thus equivariant<sup>14</sup> to translations and rotations and is therefore  $\text{Spin}(n, 0, 1)$  equivariant.  $\square$

Similar to the Euclidean case, we obtain full  $\text{Pin}(n, 0, 1)$  equivariance via multiplication with a pseudoscalar. We thus also use the EquiJoin from Eq. (7) in the projective case.

### A.3 Expressivity

As also noted in Ref. [16], in the projective algebra, the geometric product itself is unable to compute many quantities. It is thus insufficient to build expressive networks. This follows from the fact that the geometric product preserves norms.

<sup>14</sup>The authors agree with the reader that there must be an easier way to prove this.

**Lemma 7.** For the algebra  $\mathbb{G}_{n,0,r}$ , for multivectors  $x, y$ , we have  $\|xy\| = \|x\| \|y\|$ .

*Proof.*  $\|xy\|^2 = xy\tilde{xy} = xy\tilde{y}x = x\|y\|^2\tilde{x} = x\tilde{x}\|y\|^2 = \|x\|^2\|y\|^2$   $\square$

Hence, any null vector in the algebra can never be mapped to a non-null vector, including scalars. The projective algebra can have substantial information encoded as null vector, such as the position of points. This information can never influence scalars or null vectors. For example, there is no way to compute the distance (a scalar) between points just using the projective algebra. In the GATr architecture, the input to the MLPs that operate on the scalars, or the attention weights, thus could not be affected by the null information, had we only used the geometric product on multivectors.

To address this limitation, we use besides the geometric product also the join. The join is able to compute such quantities. For example, given the Euclidean vector  $e_{12\dots n}$ , we can map a null vector  $x = e_{012\dots k}$  to a non-null vector  $x \vee e_{12\dots n} \propto e_{12\dots k}$ .

## B Architecture

In this section, we provide some details on the GATr architecture that did not fit into the main paper.

**Equivariant join** One of the primitives in GATr is the equivariant join  $\text{EquiJoin}(x, y; z)$ , which we define in Eq. (7). For  $x$  and  $y$ , we use hidden states of the neural network after the previous layer. The nature of  $z$  is different: it is a reference multivector and only necessary to ensure that the function correctly changes sign under mirrorings of the inputs. We find it beneficial to choose this reference multivector  $z$  based on the input data rather than the hidden representations, and choose it as the mean of all inputs to the network.

**Auxiliary scalars** In addition to multivector representations, GATr supports auxiliary scalar representations, for instance to describe non-geometric side information such as positional encodings or diffusion time embeddings. In most layers, these scalar variables are processed like in a standard transformer, with two exceptions. In linear layers, we allow for the scalar components of multivectors and the auxiliary scalars to freely mix. In the attention operation, we compute attention weights as

$$\text{Softmax}_i \left( \frac{\sum_c \langle q_{i'c}^{MV}, k_{ic}^{MV} \rangle + \sum_c q_{i'c}^s k_{ic}^s}{\sqrt{8n_{MV} + n_s}} \right), \quad (11)$$

where  $q^{MV}$  and  $k^{MV}$  are query and key multivector representations,  $q^s$  and  $k^s$  are query and key scalar representations,  $n_{MV}$  is the number of multivector channels, and  $n_s$  is the number of scalar channels.

## C Experiments

Finally, we describe our experiments on  $n$ -body modelling and robotic planning in detail.

### C.1 Planet trajectory prediction

**Dataset** We generate a synthetic  $n$ -body dataset for  $n$  objects by following these steps for each sample:

1. The masses of  $n$  objects are sampled from log-uniform distributions. For one object (the star), we use  $m_0 \in [1, 10]$ ; for the remaining objects (the planets), we use  $m_i \in [0.01, 0.1]$ . (Following common practice in theoretical physics, we use dimensionless quantities such that the gravitational constant is 1.)
2. The initial positions of all bodies are sampled. We first use a heliocentric reference frame. Here the initial positions of all bodies are sampled. The star is set to the origin, while the planets are sampled uniformly on a plane within a distance  $r_i \in [0.1, 1.0]$  from the star.
3. The initial velocities are sampled. In the heliocentric reference frame, the star is at rest. The planet velocities are determined by computing the velocity of a stable circular orbit corresponding to the initial positions and masses, and then adding isotropic Gaussian noise (with standard deviation 0.01) to it.

Parameter	GATr	Transformer	MLP
Layers	10 blocks	10 blocks	10 layers
Channels	16 multivectors + 128 scalars	384	384
Attention heads	8	8	n/a
Parameters [ $10^6$ ]	1.9	11.8	1.3

Table 3: Hyperparameters used in the  $n$ -body experiments.

4. We transform the positions and velocities from the heliocentric reference frame to a global reference frame by applying a random translation and rotation to it. The translation is sampled from a multivariate Gaussian with standard deviation 20 and zero mean (except for the domain generalization evaluation set, where we use a mean of  $(200, 0, 0)^T$ ). The rotation is sampled from the Haar measure on  $SO(3)$ . In addition, we apply a random permutation of the bodies.
5. We compute the final state of the system by evolving it under Newton’s equations of motion, using Euler’s method and 100 time steps with a time interval of  $10^{-4}$  each.
6. Finally, samples in which any bodies have traveled more than a distance of 2 (the diameter of the solar system) are rejected. (Otherwise, rare gravitational slingshot effects dominate the regression loss and all methods become unreliable.)

We generate training datasets with  $n = 4$  and between 100 and  $10^5$  samples; a validation dataset with  $n = 4$  and 5000 samples; a regular evaluation set with  $n = 4$  and 5000 samples; a number-generalization evaluation set with  $n = 6$  and 5000 samples; and a  $E(3)$  generalization set with  $n = 4$ , an additional translation (see step 4 above), and 5000 samples.

All models are tasked with predicting the final object positions given the initial positions, initial velocities, and masses.

**Models** Our GATr model is explained in 3. We embed object masses as scalars, positions as trivectors, and velocities (like translation vectors) as bivectors.

For the Transformer baseline, we follow a pre-layer normalization [1, 46] architecture with GELU activations [23] in the MLP block. In addition, we compare to a simple MLP, also with GELU activations.

In Tbl. 4 we show hyperparameter choices and parameter counts.

**Training** All models are trained by minimizing a  $L_2$  loss on the final position of all objects. We train for 50 000 steps with the Adam optimizer, using a batch size of 64 and exponentially decaying the learning rate from  $3 \cdot 10^{-4}$  to  $3 \cdot 10^{-6}$ .

## C.2 Robotic planning through invariant diffusion

**Environment** We use the block stacking environment from Janner et al. [27]. It consists of a Kuka robotic arm interacting with four blocks on a table, simulated with PyBullet [13]. The state consists of seven robotic joint angles as well as the positions and orientations of the four blocks. We consider the task of stacking four blocks on top of each other in any order. The reward is the stacking success probability and is normalized such that 0 means that no blocks are ever successfully stacked, while 100 denotes perfect block stacking.

**Dataset and data parameterization** We train models on the offline trajectory dataset published by Janner et al. [27]. It consists of 11 000 expert demonstrations.

To describe the problem in terms of geometric quantities, we re-parameterize the environment state into the positions and orientations of the robotic endeffector as well as the four blocks. The orientations of all objects are given by two direction vectors. In addition, there are attachment variables that characterize whether the endeffector is in contact with either of the four blocks. In this parameterization, the environment state is 49-dimensional.

Parameter	GATr-Diffuser	Transformer-Diffuser	Diffuser
Transformer blocks	{10, <b>20</b> , 30}	{10, <b>20</b> , 30}	n/a
Channels	16 multivectors + 128 scalars	{ <b>144</b> , 384}	n/a
Attention heads	8	8	n/a
Parameters [ $10^6$ ]	{2.1, <b>4.0</b> , 5.9}	{1.8, ..., <b>3.5</b> , ..., 35.7}	65.1

Table 4: Hyperparameters used in the robotic planning experiments. For GATr-Diffuser and the Transformer-Diffuser, we experimented with different depth and (for the Transformer-Diffuser) channel counts. For each model, we independently chose the best-performing setting, shown here in bold. The Diffuser model uses a substantially different architecture based on a U-net, we refer the reader to Janner et al. [27] for details.

We train models in this geometric parameterization of the problem. To map back to the original parameterization in terms of joint angles, we use a simple inverse kinematics model that solves for the joint angles consistent with a given endeffector pose.

**Models** Our GATr model is explained in Sec. 3. We use the axial version, alternating between attending over time steps and over objects. We embed object positions as trivectors, object orientations as oriented planes, gripper attachment variables as scalars, and the diffusion time as scalars.

For the Transformer baseline, we follow a pre-layer normalization [1, 46] architecture with GELU activations [23] in the MLP block and rotary positional embeddings [41]. For the Diffuser baseline, we follow the architecture and hyperparameters described by Janner et al. [27].

For all models, we use the diffusion time embedding of Ref. [27]. In Tbl. 4 we show hyperparameter choices and parameter counts.

All models are embedded in a diffusion pipeline as described by Ho et al. [25], using the hyperparameter choices of Ref. [27]. In particular, we use univariate Gaussian base densities and 1000 diffusion steps.

**Training** We train all models by minimizing the simplified diffusion loss proposed by Ho et al. [25]. For our GATr models and the Diffuser baselines we use an  $L_2$  loss and train for 200 000 steps with the Adam optimizer, exponentially decaying the learning rate from  $3 \cdot 10^{-4}$  to  $3 \cdot 10^{-6}$ . This setup did not work well for the Diffuser model, where (following Janner et al. [27]) we use a  $L_1$  loss and a low constant learning rate instead.

**Evaluation** All models are evaluated by rolling out at least 200 episodes in a block stacking environment and reporting the mean task and the standard error. We use the planning algorithm and parameter choices of Janner et al. [27] (we do not optimize these, as our focus in this work is on architectural improvements). It consists of sampling trajectories of length 128 from the model, conditional on the current state; then executing these in the environment using PyBullet’s PID controller. Each rollout consists of three such phases.